

Synthesis, Structures, and Reactivity of the First Silylene-Linked Cyclopentadienyl-Phosphido Lanthanide Complexes

Olivier Tardif, Zhaomin Hou,* Masayoshi Nishiura, Take-aki Koizumi, and Yasuo Wakatsuki*

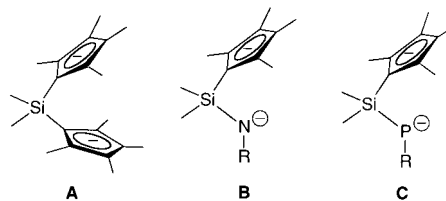
Organometallic Chemistry Laboratory, RIKEN (The Institute of Physical and Chemical Research), Hirosawa 2-1, Wako, Saitama 351-0198, Japan

Received June 4, 2001

Reaction of KPHAr (Ar = C₆H₂BU₃-2,4,6) with 1 equiv of Me₂SiCl(C₅Me₄H) in THF afforded Me₂Si(C₅Me₄H)(PHAr) (**1**) in 92% isolated yield. Metalation of **1** with 2 equiv of BuLi in THF followed by metathesis reaction with tBuOK gave the corresponding potassium complex [Me₂Si(C₅Me₄)(PHAr)K₂(thf)₄]₂ (**2**) in 88% isolated yield. Reactions of **2** with 2 equiv of LnI₂(thf)₂ in THF afforded the corresponding lanthanide(II) complexes Me₂Si(C₅Me₄)(PHAr)Ln(thf)₃ (Ln = Sm (**3**, 66%), Yb (**4**, 81%)). Two of the three thf ligands in **3** could be removed under vacuum to give [Me₂Si(C₅Me₄)(PHAr)Sm(thf)] (**3'**). Treatment of **3** with hexamethylphosphoric triamide (hmpa) or dimethoxyethane (dme) yielded the corresponding hmpa- or dme-coordinated complex Me₂Si(C₅Me₄)(PHAr)Sm(hmpa)₂ (**5**) or Me₂Si(C₅Me₄)(PHAr)Sm(dme)₂ (**6**), respectively. The reaction of 2 equiv of **3** or **3'** with benzophenone in THF afforded the corresponding disamarium(III) benzophenone-dianion complex [Me₂Si(C₅Me₄)(PHAr)Sm(thf)]₂(μ-η²-OCPh₂) (**7**). Treatment of **3** or **3'** with ICH₂CH₂I in toluene easily afforded the corresponding samarium(III) iodide complex [Me₂Si(C₅Me₄)(PHAr)Sm(μ-I)(thf)]₂ (**8**). The solid structures of all of these compounds, **1–8**, have been determined by X-ray analyses. The mono(thf)-coordinated Sm(II) complex **3'** was active for the polymerization of ethylene, ε-caprolactone, and 1,3-butadiene under appropriate conditions.

Introduction

Since the discovery of the Kaminsky metallocene catalysts in 1980, extensive studies on the design and application of organometallic complexes as polymerization catalysts have been carried out.¹ Today, the search for well-defined metal complexes with new ligand systems toward the development of more efficient, more selective catalyst families continues to attract intensive attention from both academic and industrial researchers. In this development, group 3 and 4 metal complexes bearing the silylene-linked cyclopentadienyl-amido ligands (type **B**) have received much current interest owing to their electronically more unsaturated and sterically more accessible properties than those of the metallocene analogues (e.g., type **A**).² In contrast, however, the analogous linked cyclopentadienyl-phosphido complexes (type **C**) have very hardly been explored, although this type of phosphido complex is of much interest in comparison with the amido analogues. It was previously claimed in a patent that the silylene-linked cyclopentadienyl-phosphido complexes Me₂Si(C₅Me₄)(PPh)MCl₂ (M = Ti or Zr) were formed in the reactions of Li₂[Me₂Si(C₅Me₄)(PPh)] with MCl₄, but no



spectroscopic or analytical data were given to support this assumption.³ A more recent report showed that similar reactions of Li₂[Me₂Si(C₅Me₄)(PR)] (R = cyclohexyl or C₆H₂Me₃-2,4,6) with ZrCl₄ did not give the expected cyclopentadienyl-phosphido complexes, but instead led to P–Si bond cleavage of the ligands.⁴ As far as we are aware, a structurally characterized, silylene-linked cyclopentadienyl-phosphido complex has never been reported to date for any metal.⁵ In this paper, we report the synthesis, structures, and preliminary reaction studies of the first linked cyclopentadienyl-phosphido lanthanide complexes. The synthesis

(1) Recent reviews leading to references: (a) *Chem. Rev.* **2000**, *100*, 1167–1645 (a special thematic issue on metal-catalyzed polymerization). (b) Togni, A.; Halterman, R. L. *Metallocenes*; Wiley-VCH: Weinheim, Germany, 1998; Vols. 1–2.

(2) Reviews: (a) McKnight, A. L.; Waymouth, R. M. *Chem. Rev.* **1998**, *98*, 2587. (b) Okuda, J.; Eberle, T. In *Metallocenes*; Togni, A., Halterman, R. L., Eds.; Wiley-VCH: Weinheim, Germany, 1998; Vol. 1, p 415.

(3) Stevens, J. C.; Timmers, F. J.; Wilson, D. R.; Schmidt, G. F.; Nickias, P. N.; Rosen, R. K.; Knight, G. W.; Lai, S. (Dow) Eur. Pat. Appl. 0 416 815 A2, 1991.

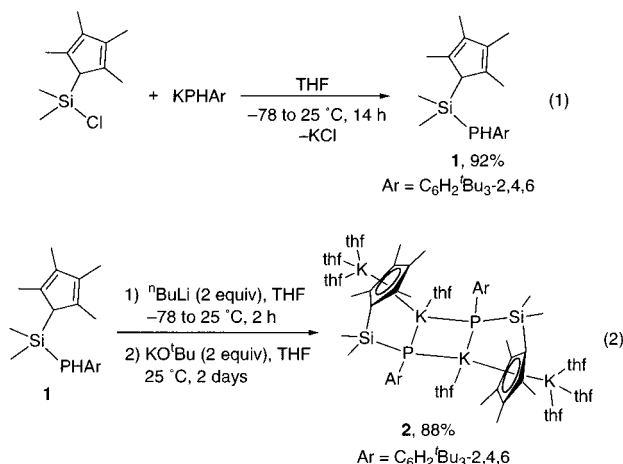
(4) Koch, T.; Blaurock, S.; Somoza, F. B.; Voigt, A.; Kirmse, R.; Hey-Hawkins, E. *Organometallics* **2000**, *19*, 2556.

(5) Formation of the dilithium salts of linked cyclopentadienyl-phosphido ligands was reported.^{3,4,5a–c} Methylene-linked cyclopentadienyl-phosphido titanium and zirconium complexes were also reported very recently.^{5d} (a) Koch, T.; Hey-Hawkins, E. *Polyhedron* **1999**, *18*, 2113. (b) Izod, K. *Adv. Inorg. Chem.* **2000**, *50*, 33. (c) Bildmann, U. J.; Muller, G. *Z. Naturforsch.* **2000**, *55*, 895. (d) Kunz, K.; Erker, G.; Döring, S.; Fröhlich, R.; Kehr, G. *J. Am. Chem. Soc.* **2001**, *123*, 6181.

and X-ray structures of the ligand and its potassium salt are also described.

Results and Discussion

Ligand Synthesis and Potassium Complex Formation. Our initial interest in linked cyclopentadienyl-phosphido lanthanide complexes stemmed originally from our studies on lanthanide complexes bearing mixed (unlinked) C_5Me_5/ER ligands (ER = a monodentate anionic ligand such as an aryloxy, thiolate, amido, phosphido, or alkyl group).⁶ In relation to the phosphido ligand that was used in a previous study,^{6d} we chose $C_6H_2^tBu_3-2,4,6$ as a substituent on the P atom for our linked cyclopentadienyl-phosphido ligand. The reaction of $KPHAr^{7a}$ with 1 equiv of $Me_2SiCl(C_5Me_4H)$ in THF readily afforded the expected secondary phosphine $Me_2Si(C_5Me_4H)PHAr$ (**1**, $Ar = C_6H_2^tBu_3-2,4,6$) as colorless crystals in 92% yield (eq 1). Metalation of **1** with 2 equiv of $BuLi$ in THF followed by metathesis reaction with $tBuOK$ gave the corresponding dipotassium cyclopentadienyl-phosphido complex $[Me_2Si(C_5Me_4)(PAr)K_2(thf)_4]_2$ (**2**) in 88% isolated yield (eq 2).



An X-ray analysis has shown that the structure of **1** is highly distorted because of the steric repulsion between the bulky aryl group and the whole silyl unit on the P atom (Figure 1 and Table 1). To reduce the repulsion, the C_5Me_4H group is oriented away from the Ar group, while one of the two methyl groups on the Si atom, C(11), is placed between the two *ortho*- tBu groups of the Ar unit and directed almost parallel along the C(12)–P(1) bond (cf. C(11)–Si(1)–P(1)–C(12) torsion angle: $9.8(2)^\circ$). As a consequence, the C(11) methyl carbon on the Si atom is as close as 3.26 Å to the *ipso*-carbon C(12) of the Ar group, and the distance of the C(10) methyl carbon on the Si atom to the C(19) methyl

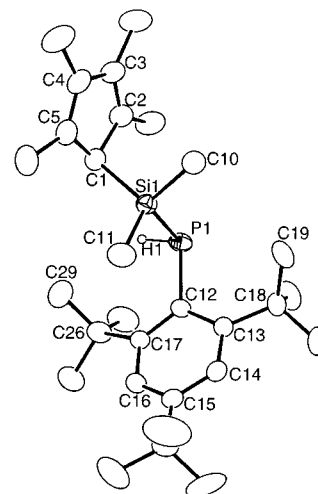


Figure 1. ORTEP drawing of **1** with 30% thermal ellipsoids. Selected bond lengths (Å) and angles (deg): P1–H1, 1.24(6); P1–Si1, 2.310(2); P1–C12, 1.856(4); H1–P1–C12, 102(2); H1–P1–Si1, 96(3); Si1–P1–C12, 100.5(1); P1–Si1–C1, 107.3(1); C1...C29, 3.84; C10...C19, 3.46; C11...C12, 3.26; C10...C12, 4.46; C11–Si1–P1–C12, $-9.8(2)$; C10–Si1–P1–C12, $110.8(2)$.

carbon of an *ortho*- tBu group in the Ar unit is as short as 3.46 Å. These distances are much shorter than the sum of the van der Waals radius of a methyl group (2.0 Å),⁸ and considerable van der Waals repulsion between the Ar unit and the substituents on the Si atom must be present. Because of this repulsion, the C(12) atom is no longer coplanar with the other five carbon atoms C(13–17) in the phenyl ring of the Ar group (cf. C(12)···(13–17) plane: $0.194(5)$ Å), and the P(1) atom is further out of the plane, with the distance of P(1) to the C(13–17) plane being as long as $0.873(7)$ Å (cf. Table 1 and Figure 1).

Orange crystals of **2** suitable for diffraction studies were obtained from a concentrated THF solution. An X-ray analysis established that one of the two K atoms, K(1), is chelated by the Cp'-phosphido ligand, while the other K atom (K(2)) is bonded to the other side of the Cp' unit ($Cp' = C_5Me_4$) (Figure 2). The whole molecule adopts a dimeric structure through "intermolecular" interaction between the chelated K(1) atom and the P atom, with a crystallographic inversion center being present at the center of the molecule. As compared with **1**, the chelation of the Cp'-phosphido ligand to the potassium atom in **2** further increased the steric repulsion between the methyl groups on the Si atom and the *ortho*- tBu groups in the aryl unit (cf. Table 1 and Figure 2). Therefore, the P(1) and C(12) atoms in **2** were further dragged out of the C(13–17) plane, with the distances of P(1) and C(12) to the C(13–17) plane being increased to $1.10(2)$ and $0.24(1)$ Å, respectively. The average bond distance of the chelating K(1)–Cp' bonds ($3.049(8)$ Å) is slightly longer than that of the K(2)–Cp' bonds ($2.987(8)$ Å). But, both can be compared with that of the K–Cp* bonds found in $[(Cp^*K(Py)_2)]_n$ ($Cp^* = C_5Me_5$, $Py = pyridine$) ($3.030(2)$ Å).⁹ The K(1)–P(1) bond distance ($3.324(4)$ Å) in **2** is significantly shorter than that of the K(1)–P(1*) bond ($3.430(3)$ Å), but is in the 3.181 – 3.345

(6) (a) Hou, Z.; Zhang, Y.; Tardif, O.; Wakatsuki, Y. *J. Am. Chem. Soc.* **2001**, *123*, 9216. (b) Hou, Z.; Kaita; S. Wakatsuki, Y. *Pure Appl. Chem.* **2001**, *73*, 291. (c) Hou, Z. *J. Synth. Org. Chem. Jpn.* **2001**, *59*, 82. (d) Hou, Z.; Zhang, Y.; Tezuka, H.; Xie, P.; Tardif, O.; Koizumi, T.; Yamazaki, H.; Wakatsuki, Y. *J. Am. Chem. Soc.* **2000**, *122*, 10533. (e) Hou, Z.; Wakatsuki, Y. *J. Alloys Compd.* **2000**, *303–304*, 75. (f) Zhang, Y.; Hou, Z.; Wakatsuki, Y. *Macromolecules* **1999**, *32*, 939. (g) Hou, Z.; Tezuka, H.; Zhang, Y.; Yamazaki, H.; Wakatsuki, Y. *Macromolecules* **1998**, *31*, 8650. (h) Zhang, Y.; Hou, Z.; Wakatsuki, Y. *Bull. Chem. Soc. Jpn.* **1998**, *71*, 1381. (i) Hou, Z.; Zhang, Y.; Yoshimura, T.; Wakatsuki, Y. *Organometallics* **1997**, *16*, 2963.

(7) (a) Rabe, G.; Yap, G. P. A.; Rheingold, A. L. *Inorg. Chem.* **1997**, *36*, 1990. (b) Frenzel, C.; Jörchel, P.; Hey-Hawkins, E. *Chem. Commun.* **1998**, 1363.

(8) Pauling, L. *The Nature of the Chemical Bond*, 3rd ed.; Cornell University Press: Ithaca, NY, 1960; pp 260–261.

Table 1. Summary of Selected Distances (Å) and Angles (deg) for the Silylene-Linked Cyclopentadienyl-Phosphido Complexes of Type D (see also Figures 1–7)

	1	2	4	5	6 (two molecules)	7	8
M =	H	K	Yb(II)	Sm(II)	Sm(II)	Sm(III)	Sm(III)
M–Cp'(av)		3.049(8)	2.72(1)	2.796(7)	2.858(5), 2.848(6)	2.708(3)	2.690(7)
M–Cp'(centrd)		2.802	2.43	2.525	2.594, 2.581	2.426	2.402
M–P	1.24(6)	3.324(4)	2.851(4)	3.041(2)	2.977(2), 2.973(2)	2.7962(9)	2.720(2)
P–Si	2.310(2)	2.232(3)	2.198(5)	2.238(3)	2.212(2), 2.213(2)	2.211(1)	2.195(3)
P–C1	1.856(4)	1.895(8)	1.87(1)	1.869(6)	1.864(6), 1.866(6)	1.877(3)	1.868(8)
P⋯plane(C _{2–6})	0.873(7)	1.10(2)	1.09(4)	1.10(1)	1.10(2), 0.85(2)	1.35(2)	1.08(2)
Cl⋯plane(C _{2–6})	0.194(5)	0.24(1)	0.24(3)	0.26(1)	0.24(1), 0.19(1)	0.27(1)	0.22(1)
Me1⋯Bu1	3.84	3.48	3.46	3.79	3.53, 3.49	3.55	3.44
Me2⋯Bu2	3.46	3.62	3.38	3.58	3.42, 3.47	3.58	3.64
Me1⋯C1	3.26	4.15	3.89	3.38	3.59, 4.00	3.93	4.17
Me2⋯C1	4.46	3.44	3.83	4.41	4.05, 4.11	3.90	3.88
Me1–Si–P–C1	9.8(2)	84.4(5)	59(1)	19.3(5)	44.7(4), 53.6(4)	60.3(4)	70.2(6)
Me2–Si–P–C1	110.8(2)	30.3(5)	61(1)	98.7(4)	72.3(4), 65.4(4)	58.9(4)	51.2(5)
∠Cp'(centrd)–M–P		86.8	96.4	93.0	92.5, 91.6	95.3	96.0
∠M–P–C1	102(2)	144.8(3)	168.7(4)	128.7(2)	161.1(2), 160.5(2)	164.4(1)	156.0(3)
∠M–P–Si	96(3)	85.8(1)	88.4(2)	85.37(8)	89.51(7), 90.83(7)	91.37(4)	92.9(1)
∠Si–P–C1	100.5(1)	99.3(2)	102.5(4)	102.3(2)	101.0(2), 107.4(2)	103.2(1)	107.6(1)
Σ of angles around P	298.5	329.9	359.6	316.4	351.1, 358.7	359.0	356.5

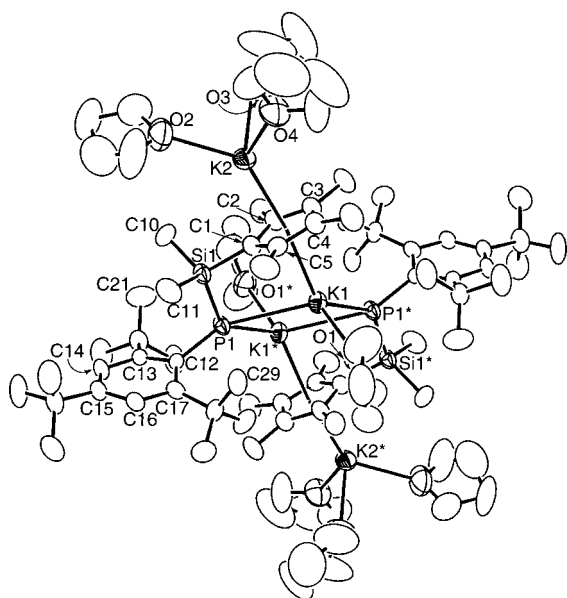
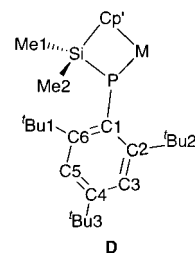


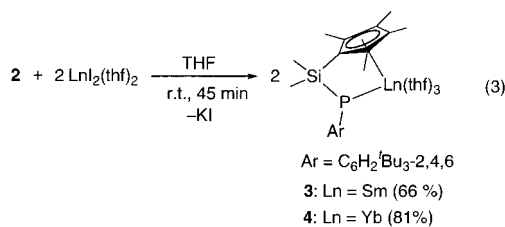
Figure 2. ORTEP drawing of **2** with 30% thermal ellipsoids. Selected bond lengths (Å) and angles (deg): K1–C1, 2.953(8); K1–C2, 3.016(9); K1–C3, 3.114(8); K1–C4, 3.126(8); K1–C5, 3.037(7); K2–C1, 2.959(7); K2–C2, 2.979(7); K2–C3, 3.034(8); K2–C4, 3.02(1); K2–C5, 2.944(8); K1–P1, 3.324(4); K1–P1*, 3.432(2); K1–O1, 2.714(8); K2–O2, 2.72(1); K2–O3, 2.72(1); K2–O4, 2.728(9); P1–Si1, 2.232(3); P1–C12, 1.895(8); Cp'(centroid)–K1–P1, 86.7; Cp'(centroid)–K1–1*, 126.7; Cp'(centroid)–K1–1, 115.3; P1–K1–P1*, 106.53(7); K1–P1–K1*, 73.47(7); K1–Cp'(centroid)–K2, 172.9; O2–K2–Cp'(centroid), 135.0; O3–K2–Cp'(centroid), 117.6; O4–K2–Cp'(centroid), 121.2; O2–K2–O3, 85.3(4); O2–K2–O4, 96.8(4); O3–K2–O4, 86.6(4); K1–P1–C12, 144.8(3); K1–P1–Si1, 85.8(1); Si1–P1–C12, 99.3(2); C10⋯C21, 3.48; C11⋯C29, 3.62; C10⋯C12, 4.15; C11⋯C12, 3.44; C10–Si1–P1–C12, –84.4(5); C11–Si1–P1–C12, 30.3(5).

Å range reported for the K–P bonds in the polymeric potassium phosphido compounds [KPH(C₆H₂Me₃-2,4,6)]_n^{7a} and [K₃(thf)₂{PH(C₆H₂Me₃-2,4,6)}₃]_n^{7b}

Lanthanide(II) Complexes. Despite the intense distortion in the ligand, metathetical reactions of the potassium complex **2** with 2 equiv of LnI₂(thf)₂ in THF

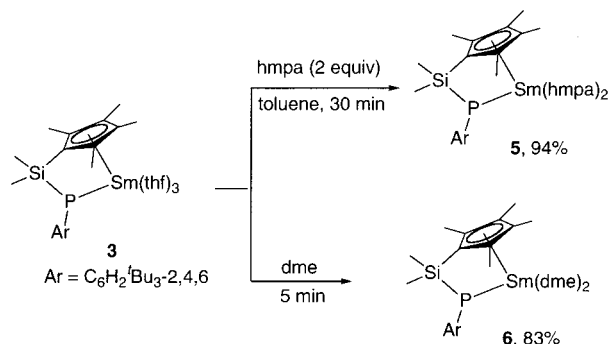


easily afforded the corresponding Cp'-phosphido lanthanide(II) complexes Me₂Si(C₅Me₄)(PAr)Ln(thf)₃ (Ar = C₆H₂Bu₃-2,4,6; Ln = Sm (**3**), Yb (**4**)) in good yields (eq 3). Two of the three thf ligands in **3** could be removed



under vacuum to give the monosolvated Sm(II) complex [Me₂Si(C₅Me₄)(PAr)Sm(thf)] (**3**). Treatment of **3** with hexamethylphosphoric triamide (hmpa) or dimethoxyethane (dme) yielded the corresponding hmpa- or dme-coordinated complex, **5** or **6**, respectively (Scheme 1).

Scheme 1



The three thf ligands in the Yb(II) complex **4** could be easily removed by dissolving **4** in toluene followed by

(9) Rabe, G.; Roesky, H. W.; Stalke, D.; Pauer, F.; Sheldrick, G. M. *J. Organomet. Chem.* **1991**, *403*, 11.

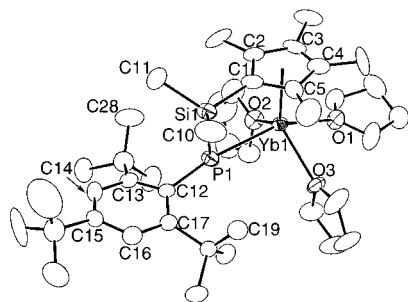


Figure 3. ORTEP drawing of **4** with 30% thermal ellipsoids. Selected bond lengths (Å) and angles (deg): Yb1–P1, 2.851(4); Yb1–C1, 2.64(1); Yb1–C2, 2.70(1); Yb1–C3, 2.77(1); Yb1–C4, 2.80(2); Yb1–C5, 2.71(1); Yb1–O1, 2.535(9); Yb1–O2, 2.425(9); Yb1–O3, 2.469(9); P1–Si1, 2.198(5); P1–C12, 1.87(1); Cp'(centroid)–Yb1–P1, 96.4; Cp'(centroid)–Yb1–O1, 107.2; Cp'(centroid)–Yb1–O2, 122.0; Cp'(centroid)–Yb1–O3, 125.0; P1–Yb1–O1, 156.3(2); P1–Yb1–O2, 92.4(3); P1–Yb1–O3, 92.7(3); O1–Yb1–O2, 76.73(3); O1–Yb1–O3, 72.6(3); O2–Yb1–O3, 111.6(4); Yb1–P1–C12, 168.7(4); Yb1–P1–Si1, 88.4(2); Si1–P1–C12, 102.5(4); C11...C28, 3.46; C10...C19, 3.38; C11...C12, 3.89; C10...C12, 3.83; C11–Si1–P1–C12, –59(1); C10–Si1–P1–C12, 61(1).

evaporation of the solvent under vacuum, which yielded the unsolvated complex $[\text{Me}_2\text{Si}(\text{C}_5\text{Me}_4)(\text{PAr})\text{Yb}]$ (**4**).

Orange needlelike single crystals of **4** were obtained from a saturated THF solution. An X-ray analysis showed that **4** adopts a monomeric structure, in which the Yb(II) center is bonded to one chelating Cp'-phosphido ligand and three thf terminal ligands (Figure 3). The average Yb–C(Cp') bond distance in **4** (2.72 Å) is significantly longer than that found in the analogous Cp'-anilido ytterbium(II) complex $\text{Me}_2\text{Si}(\text{C}_5\text{Me}_4)(\text{NPh})\text{Yb}(\text{thf})_3$ (2.65 Å),¹⁰ while the Yb–P bond distance in **4** (2.851(4) Å) is much shorter than those reported for the bis(phosphido) ytterbium(II) complexes such as Yb(PHC₆H₂Bu₃-2,4,6)₂(thf)₄ (3.025(2) Å),^{11a} Yb(PPh₂)₂(thf)₄ (2.991(2) Å),^{11b} Yb{P(C₆H₃OMe-2-Me-3)CH(SiMe₃)₂}₂(thf)₂ (2.969(3) Å),^{11c} and Yb{P(C₆H₂Me₃-2,4,6)₂}₂(thf)₄ (2.925(2) Å).^{11d} The ∠P–Yb–Cp'(centroid) angle in **4** (96.4°) is comparable with the ∠N–Yb–Cp'(centroid) angle in $\text{Me}_2\text{Si}(\text{C}_5\text{Me}_4)(\text{NPh})\text{Yb}(\text{thf})_3$ (95°).¹⁰

Although the X-ray structure of the thf-coordinated Sm(II) complex **3** could not be satisfactorily refined owing to poor quality of the crystal, the connectivity of the molecule, which is similar to that of the Yb(II) analogue **4**, was unambiguously determined.¹² The structures of the hmpa-coordinated Sm(II) complex **5** (Figure 4) and its dme analogue **6** (Figure 5) could be well refined. In the case of **6**, two independent molecules were found in the unit cell. The average Sm–C(Cp') bond distance in **5** (2.796(7) Å) is shorter than those in **6** (2.858(5), 2.848(6) Å) and those of the Sm–C(Cp*) bonds found in the unlinked half-metallocene Sm(II) complexes such as Cp*Sm(N(SiMe₃)₂)(hmpa)₂ (2.86(2)

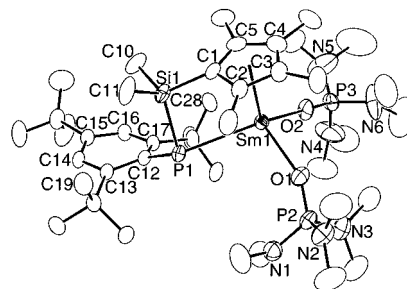


Figure 4. ORTEP drawing of **5** with 30% thermal ellipsoids. Selected bond lengths (Å) and angles (deg): Sm1–P1, 3.041(2); Sm1–C1, 2.740(6); Sm1–C2, 2.741(6); Sm1–C3, 2.810(7); Sm1–C4, 2.879(8); Sm1–C5, 2.812(8); Sm1–O1, 2.456(5); Sm1–O2, 2.476(5); P1–Si1, 2.238(3); P1–C12, 1.869(6); Cp'(centroid)–Sm1–P1, 93.04; Cp'(centroid)–Sm1–O1, 113.0; Cp'(centroid)–Sm1–O2, 116.9; Sm1–P1–C12, 128.7(2); Sm1–P1–Si1, 85.37(8); Si1–P1–C12, 102.3(2); P1–Sm1–O1, 101.2; P1–Sm1–O2, 135.7(1); O1–Sm1–O2, 96.2(2); C10...C28, 3.79; C11...C19, 3.58; C10...C12, 3.38; C11...C12, 4.41; C10–Si1–P1–C12, –19.3(5); C11–Si1–P1–C12, 98.7(4).

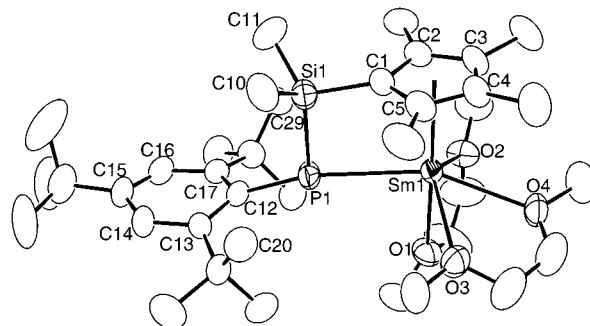


Figure 5. ORTEP drawing of **6** with 30% thermal ellipsoids. Only one of the two independent molecules is shown. Selected bond lengths (Å) and angles (deg): Sm1–P1, 2.977(2); Sm1–C1, 2.778(5); Sm1–C2, 2.848(5); Sm1–C3, 2.934(5); Sm1–C4, 2.917(5); Sm1–C5, 2.816(5); Sm1–O1, 2.740(5); Sm1–O2, 2.575(5); Sm1–O3, 2.601(6); Sm1–O4, 2.645(6); P1–Si1, 2.212(2); P1–C12, 1.864(6); Cp'(centroid)–Sm1–P1, 92.5; Cp'(centroid)–Sm1–O1, 177.3; Cp'(centroid)–Sm1–O2, 116.9; Cp'(centroid)–Sm1–O4, 103.5; Sm1–P1–C12, 161.1(2); Sm1–P1–Si1, 89.51(7); Si1–P1–C12, 101.0(2); P1–Sm1–O1, 85.1(1); P1–Sm1–O2, 110.5(2); P1–Sm1–O3, 99.8(2); P1–Sm1–O4, 159.1(2); C11...C29, 3.53; C10...C20, 3.42; C11...C12, 3.59; C10...C12, 4.05; C11–Si1–P1–C12, –44.7(4); C10–Si1–P1–C12, 72.3(4).

Å)^{6d} and Cp*Sm(OC₆H₂Bu₂-2,6-Me-4)(hmpa)₂ (2.860(7) Å, Cp* = C₅Me₅).⁶ⁱ The Sm–P bond distance in **5** (3.041(2) Å) is, however, longer than those in **6** (2.977(2), 2.973(2) Å). The PAr unit in **5** adopts a “bent” structure (∠Sm–P–Ar: 128.7(2)°), which is in contrast with the “linear” ones in **6** (∠Sm–P–Ar: 161.1(2)°, 160.5(2)°) and **4** (∠Yb–P–Ar: 168.7(4)°) (cf. Table 1). Moreover, the sum of the bond angles around the P atom in **5** (316.4°) is much less than 360°, showing that the P atom and the atoms around it are arranged in a pyramidal form. In contrast, the analogous angle sum in **4** (359.6°) or **6** (351.1°, 358.7°) is close to 360°, which indicates that the P atom and the atoms around it in **4** and **6** are almost coplanar. These results suggest that the donation of the lone electron pair on the P atom to the central metal ion in **5** is not as sufficient as that in **4** and **6**, probably

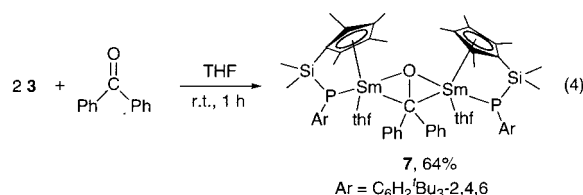
(10) Hou, Z.; Koizumi, T.; Nishiura, M.; Wakatsuki, Y. *Organometallics* **2001**, *20*, 3323.

(11) (a) Rabe, G. W.; Guzei, I. A.; Rheingold, A. L. *Inorg. Chem.* **1997**, *36*, 4914. (b) Rabe, G. W.; Yap, G. P. A.; Rheingold, A. L. *Inorg. Chem.* **1995**, *34*, 4521. (c) Clegg, W.; Izod, K.; Liddle, S. T.; O'Shaughnessy, P.; Sheffield, J. M. *Organometallics* **2000**, *19*, 2090. (d) Atlan, S.; Nief, F.; Ricard, L. *Bull. Chim. Soc. Fr.* **1995**, *132*, 649.

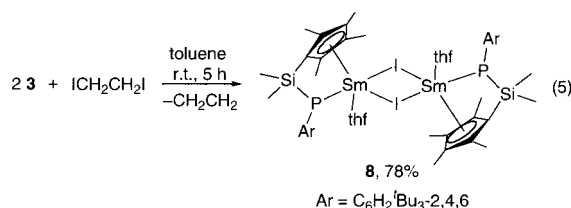
(12) Crystal data for **3**: monoclinic, space group *C2/m*, *a* = 25.414(7) Å, *b* = 14.461(6) Å, *c* = 13.977(3) Å, β = 94.101(2)°, *V* = 5123(3) Å³, *Z* = 4.

owing to the influence of the strongly electron-donating hmpa ligands in **5**.¹³ The extent of distortion in the Cp'-phosphido ligands of **4–6** is comparable with each other and also with that in **2**, in terms of the distances between the P atom or the methyl groups on the Si atom and the aryl unit (cf. Table 1).

One-Electron-Transfer Reactions of the Sm(II) Complex 3. Despite the great distortion in the structures of **2–6**, these complexes were quite stable in solid state at room temperature under an inert atmosphere. However, the lanthanide(II) complexes **3–6** gradually decomposed into yet unidentified products in a THF solution during a period of 1–3 days. Nevertheless, the reduction chemistry of such a lanthanide(II) complex (e.g., **3**) could be examined in THF or toluene. The reaction of 2 equiv of **3** or **3'** with benzophenone in THF afforded the corresponding disamarium(III) benzophenone-dianion complex **7** in 64% isolated yield (eq 4).



The use of 1 equiv of **3** in this reaction also gave **7** as the only isolable product, albeit in a lower yield, which suggests that the formation of a benzophenone-dianion species is easier than that of a ketyl species in the present reaction.^{14,15} These results are in contrast with those previously reported for the analogous reactions of lanthanide(II) complexes bearing other ligand systems such as (C₅Me₅)₂Sm(thf)₂,^{15c} Sm(OC₆H₂(Bu₃-2,4,6-Me-4)₂(thf)₂,^{15c,g} and Me₂Si(C₅Me₄)(NPh)Yb(thf)₃.¹⁰ Treatment of **3** or **3'** with ICH₂CH₂I in toluene easily afforded the corresponding samarium(III) iodide complex **8** in 78% isolated yield (eq 5). The Sm(III) complexes **7** and **8** seemed to be much more stable than the lanthanide(II) complexes **3–6** in THF solution.



The average bond distances of the Sm–C(Cp') bond (2.708(3) Å) and the Sm–P bond (2.7962(9) Å) in **7** are somewhat longer than those in **8** (Sm–C(Cp'), 2.690(7) Å; Sm–P, 2.720(2) Å), respectively. However, all of these bond distances are respectively much shorter than those

(13) Generally, HMPA is much more electron-donating than THF or DME. For examples, see: (a) Hou, Z.; Zhang, Y.; Wakatsuki, Y. *Bull. Chem. Soc. Jpn.* **1997**, *70*, 149. (b) Hou, Z.; Wakatsuki, Y. *J. Chem. Soc., Chem. Commun.* **1994**, 1205. (c) Hou, Z.; Kobayashi, K.; Yamazaki, H. *Chem. Lett.* **1991**, 265.

(14) For examples of formation and structures of ketone-dianion complexes, see: (a) Hou, Z.; Fujita, A.; Yamazaki, H.; Wakatsuki, Y. *Chem. Commun.* **1998**, 669. (b) Hou, Z.; Yamazaki, H.; Kobayashi, K.; Fujiwara, Y.; Taniguchi, H. *J. Chem. Soc., Chem. Commun.* **1992**, 722. (c) Hou, Z.; Yamazaki, H.; Fujiwara, Y.; Taniguchi, H. *Organometallics* **1992**, *11*, 2711. (d) Bogdanovic, B.; Kruger, C.; Wermeckes, B. *Angew. Chem., Int. Ed. Engl.* **1980**, *19*, 817.

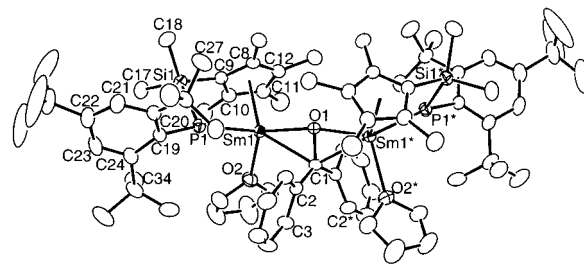


Figure 6. ORTEP drawing of **7** with 30% thermal ellipsoids. The lattice THF molecules are omitted for clarity. Selected bond lengths (Å) and angles (deg): Sm1–P1, 2.7962(9); Sm1–C8, 2.665(3); Sm1–C9, 2.658(3); Sm1–C10, 2.711(3); Sm1–C11, 2.764(3); Sm1–C12, 2.740(3); Sm1–C1, 2.584(2); Sm1–O1, 2.2932(3); Sm1–O2, 2.470(2); P1–Si1, 2.211(1); P1–C19, 1.877(3); C(1)–O(1), 1.426(4); Cp'(centroid)–Sm1–P1, 95.3; Cp'(centroid)–Sm1–O1, 109.7; Cp'(centroid)–Sm1–C1, 134.2; Cp'(centroid)–Sm1–O2, 106.3; P1–Sm1–O1, 119.54(3); P1–Sm1–O2, 106.81(6); P1–Sm1–C1, 124.154(19); Sm1–P1–C19, 164.4(1); Sm1–P1–Si1, 91.37(1); Si1–P1–C19, 107.6(1); O2–Sm1–O1, 116.54(8); O1–Sm1–C1, 33.34(9); O2–Sm1–C1, 85.39(9); Sm1–O1–Sm1*, 169.15(12); Sm1–C1–Sm1*, 124.17(15); C2–C1–O1, 116.2(2); C2–C1–C2*, 127.7(4); C17...C34, 3.55; C18...C27, 3.58; C17...C19, 3.93; C18...C19, 3.90; C17–Si1–P1–C19, –60.3(4); C18–Si1–P1–C19, 58.9(4).

in the Sm(II) complexes **5** and **6**, owing to the smaller size of Sm(III) than that of Sm(II) (Table 1).¹⁶

Complex **7** has a crystallographic 2-fold axis passing through the C(1)–O(1) bond of the benzophenone unit (Figure 6). The two Sm atoms are symmetrically bridged by the CO group of the benzophenone unit in a η²-fashion. The C(1)–O(1) bond distance in **7** (1.426(4) Å) is comparable with those reported for the benzophenone-dianion units in [Li₂(OCPh₂)(thf)(tmeda)]₂ (1.406 Å) (tmeda = tetramethylethylenediamine)^{14d} and [Yb(μ-η¹:η²-OCPh₂)(hmpa)₂]₂ (1.39(6) Å)^{14b,c} and significantly longer than that of the C–O double bond found in free benzophenone (1.23 Å).¹⁷ The distance of the bridging Sm(1)–C(1) bond in **7** (2.584(2) Å) is much longer than that reported for the terminal Sm–methyl bond in (C₅Me₅)₂SmMe(thf) (2.48(1) Å).¹⁸ Similarly, the distance of the bridging Sm(1)–O(1) bond in **7** (2.2932(3) Å) is significantly longer than those of the terminal Sm–O(diphenylmethoxy) bonds found in Sm(OCHPh₂)₂-(OAr)(hmpa)₂ (av 2.145(5) Å) (Ar = C₆H₃(Bu₂-2,6)).¹⁹ As far as we are aware, **7** represents the first example of a structurally characterized lanthanide(III) ketone-dianion complex.

Complex **8** possesses a crystallographic inversion center at the center of the molecule (Figure 7). The

(15) For examples of formation and structures of ketyl complexes, see: (a) Hou, Z.; Jia, X.; Fujita, A.; Tezuka, H.; Yamazaki, H.; Wakatsuki, Y. *Chem. Eur. J.* **2000**, *6*, 2994. (b) Hou, Z.; Fujita, A.; Koizumi, T.; Yamazaki, H.; Wakatsuki, Y. *Organometallics* **1999**, *18*, 1979. (c) Hou, Z.; Fujita, A.; Zhang, Y.; Miyano, T.; Yamazaki, H.; Wakatsuki, Y. *J. Am. Chem. Soc.* **1998**, *120*, 754. (d) Hou, Z.; Jia, X.; Wakatsuki, Y. *Angew. Chem., Int. Ed. Engl.* **1997**, *36*, 1292. (e) Clegg, W.; Eaborn, C.; Izod, K.; O'Shaughnessy, P.; Smith, J. D. *Angew. Chem., Int. Ed. Engl.* **1997**, *36*, 2815. (f) Takats, J. *J. Alloys Compd.* **1997**, *249*, 51. (g) Hou, Z.; Miyano, T.; Yamazaki, H.; Wakatsuki, Y. *J. Am. Chem. Soc.* **1995**, *117*, 4421.

(16) Shannon, R. D. *Acta Crystallogr., Sect. A* **1976**, *32*, 751.

(17) Fleischer, E. B.; Sung, N.; Hawkinson, S. *J. Phys. Chem.* **1968**, *72*, 4311.

(18) Evans, W. J.; Chamberlain, L. R.; Ulibarri, T. A.; Ziller, J. W. *J. Am. Chem. Soc.* **1988**, *110*, 6423.

(19) Hou, Z.; Yoshimura, T.; Wakatsuki, Y. *J. Am. Chem. Soc.* **1994**, *116*, 11169.

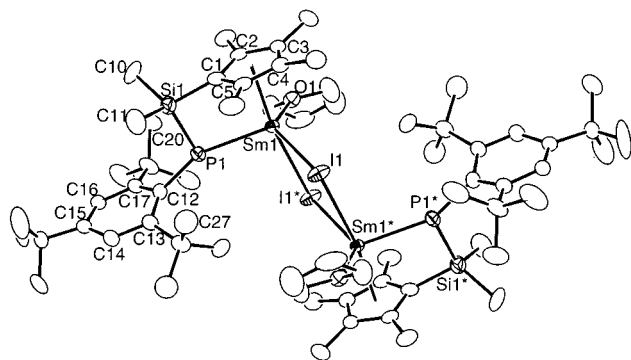


Figure 7. ORTEP drawing of **8** with 30% thermal ellipsoids. Selected bond lengths (Å) and angles (deg): Sm1–P1, 2.720(2); Sm1–C1, 2.628(7); Sm1–C2, 2.655(8); Sm1–C3, 2.713(7); Sm1–C4, 2.753(7); Sm1–C12, 2.701(7); Sm1–O1, 2.446(5); Sm1–I1, 3.1037(7); Sm1–I1*, 3.2299(7); P1–Si1, 2.195(3); P1–C12, 1.868(8); Cp'(centroid)–Sm1–P1, 96.0; Cp'(centroid)–Sm1–I1, 102.1; Cp'(centroid)–Sm1–I1*, 171.8; Cp'(centroid)–Sm1–O1, 101.0; P1–Sm1–I1, 114.51(6); P1–Sm1–I1*, 91.70(5); P1–Sm1–O1, 102.74(14); O1–Sm1–I1, 133.24(12); O1–Sm1–I1*, 74.37(12); I1–Sm1–I1*, 77.18(2); Sm1–I1–Sm1*, 102.82(2); Sm1–P1–C12, 156.0(3); Sm1–P1–Si1, 92.9(1); Si1–P1–C12, 107.6(1); C10···C20, 3.44; C11···C27, 3.64; C10···C12, 4.17; C11···C12, 3.88; C10–Si1–P1–C12, –70.2(6); C11–Si1–P1–C12, 51.2(5).

Sm(1)–I(1) bond distance (3.1037(7) Å) is significantly shorter than that of the Sm(1)–I(1*) bond (3.2299(7) Å), showing that the iodide bridges are asymmetric. These bridging Sm–I bond distances are significantly longer than those of the terminal Sm–I bonds found in (C₅Me₅)₂SmI(thf) (3.048(2) Å)²⁰ and (ArO)₂SmI(thf)₂ (3.024(2) Å) (Ar = OC₆H₂/Bu₃-2,6-Me-4).²¹

Polymerization Reactions. The polymerization of ethylene by the mono(thf)-coordinated Sm(II) complex **3'** at room temperature under 1 atm yielded extremely high molecular weight polyethylene that was insoluble in *ortho*-dichlorobenzene at 135 °C (13.6 kg polymer (mol Sm)⁻¹ h⁻¹, $M_n > 4 \times 10^6$). This result is in contrast with what was observed in the case of the analogous, less sterically demanding Cp'-anilido Sm(II) complex Me₂Si(C₅Me₄)(NPh)Sm(thf)_x ($x = 0-1$) (44.8 kg polymer (mol Sm)⁻¹ h⁻¹, $M_n = 7.26 \times 10^5$, $M_w/M_n = 1.58$)¹⁰ and the mixed C₅Me₅/PHAr-ligated Sm(II) complex [(C₅Me₅)Sm(PHAr)(thf){K(thf)(C₅Me₅)}]_n (Ar = C₆H₂/Bu₃-2,4,6) (57.6 kg polymer (mol Sm)⁻¹ h⁻¹, $M_n = 5.0 \times 10^5$, $M_w/M_n = 2.9$).^{6d} Complex **3'** seemed to react with styrene in toluene at room temperature, but no polymer product was obtained. The less reducing Yb(II) complex **4** or **4'** or the more crowded Sm(II) complexes **3**, **5**, and **6** did not show an activity for ethylene polymerization under the same conditions. Complex **3'** was also very active for the ring-opening polymerization of ϵ -caprolactone (CL), which quantitatively converted 1000 equiv of CL into poly(CL) ($M_n = 1.06 \times 10^5$, $M_w/M_n = 1.54$) at room temperature within 10 min.²² In the presence of MMAO

(MMAO = modified methylaluminoxane which contains isobutylaluminoxane) as a cocatalyst, **3'** showed high activity and 1,4-*cis* selectivity for the polymerization of 1,3-butadiene (1,4-*cis*:1,4-*trans*:1,2- = 92.8:4.0:3.2; $M_n = 3.07 \times 10^5$, $M_w/M_n = 1.99$).²³

Conclusion

We have shown that the silylene-linked cyclopentadienyl phosphido unit [Me₂Si(C₅Me₄)(PC₆H₂/Bu₃-2,4,6)]²⁻ can serve as a useful ancillary ligand system for both divalent and trivalent lanthanides. The potassium complex (**2**) and the lanthanide complexes (**3–8**) reported in this paper represent the first examples of structurally characterized, silylene-linked cyclopentadienyl-phosphido complexes. The previous lack of success in obtaining an analogous group 4 metal complex⁴ and the difference in stability among the potassium and divalent and trivalent lanthanide complexes **2–8** suggest that the stability of a silylene-linked cyclopentadienyl-phosphido complex is very dependent on the nature of the central metal ion. Preliminary reaction studies on the Sm(II) complex **3** demonstrate that the linked cyclopentadienyl-phosphido lanthanide(II) complexes can serve as a new family of reducing agents and polymerization catalysts. Studies on analogous lanthanide complexes bearing other phosphido ligands are under progress.

Experimental Section

General Methods. All reactions were carried out under a dry and oxygen-free argon atmosphere by using Schlenk techniques or under a nitrogen atmosphere in an MBraun glovebox. The argon was purified by being passed through a Dryclean column (4 Å molecular sieves, Nikka Seiko Co.) and a Gasclean GC-XR column (Nikka Seiko Co.). The nitrogen in the glovebox was constantly circulated through a copper/molecular sieves (4 Å) catalyst unit. The oxygen and moisture concentrations in the glovebox atmosphere were monitored by an O₂/H₂O Combi-Analyzer (MBraun) to ensure both were always below 1 ppm. Samples for NMR spectroscopic measurements were prepared in the glovebox by use of J. Young valve NMR tubes (Wilmad 528-JY). ¹H, ¹³C, and ³¹P NMR spectra were recorded on a JNM-EX 270 (FT, 270 MHz) spectrometer. Elemental analyses were performed by the Chemical Analysis Laboratory of RIKEN. Solvents were distilled from sodium/benzophenone ketyl, degassed by the freeze–pump–thaw method (three times), and dried over fresh Na chips in the glovebox. HMPA was distilled from Na under reduced pressure, degassed by the freeze–thaw method, and dried over molecular sieves (4 Å). (C₅Me₄H)SiMe₂Cl was purchased from Aldrich. PH₂(C₆H₂/Bu₃-2,4,6),²⁴ KPH(C₆H₂/Bu₃-2,4,6),^{7a} and LnI₂(thf)₂²⁵ (Ln = Sm, Yb) were prepared according to literature methods.

Me₂Si(C₅Me₄H)PH(C₆H₂/Bu₃-2,4,6) (1). KPH(C₆H₂/Bu₃-2,4,6) (4.25 g, 13.43 mmol) in THF (50 mL) was added dropwise at –78 °C to a THF solution (50 mL) of Me₂SiCl(C₅Me₄H) (2.97 g, 13.83 mmol). The reaction mixture was then warmed to room temperature and stirred for 14 h. Removal of the THF under vacuum afforded a white residue, which was then

(20) Evans, W. J.; Grate, J. W.; Levan, K. R.; Bloom, I.; Peterson, T. T.; Doedens, R. J.; Zhang, H.; Atwood, J. L. *Inorg. Chem.* **1986**, *25*, 3614.

(21) Hou, Z.; Fujita, A.; Yoshimura, T.; Jesorka, A.; Zhang, Y.; Yamazaki, H.; Wakatsuki, Y. *Inorg. Chem.* **1996**, *35*, 7190.

(22) For examples of the ring-opening polymerization of lactones by Sm(II) complexes, see: (a) Nishiura, M.; Hou, Z.; Koizumi, T.; Imamoto, T.; Wakatsuki, Y. *Macromolecules* **1999**, *32*, 8245. (b) Evans, W. J.; Katsumata, H. *Macromolecules* **1994**, *27*, 2330.

(23) For stereospecific 1,4-*cis*, living polymerization of 1,3-butadiene by samarocene-based catalysts, see: (a) Kaita, S.; Hou, Z.; Wakatsuki, Y. *Macromolecules* **1999**, *32*, 9078. (b) Kaita, S.; Hou, Z.; Wakatsuki, Y. *Macromolecules* **2001**, *34*, 1538.

(24) Cowley, A. H.; Norman, N. C.; Pakulski, M.; Becker, G.; Layh, M.; Kirchner, E.; Schmidt, M. *Inorg. Synth.* **1990**, *27*, 235.

(25) Watson, P. L.; Tulip, T. H.; Williams, I. *Organometallics* **1990**, *9*, 1999.

extracted with hexane. The volatiles were removed under reduced pressure to yield **1** as a white crystalline powder (5.63 g, 12.33 mmol, 92% yield). Colorless blocks of **1** suitable for X-ray analysis were obtained from a concentrated hexane solution. $^1\text{H NMR}$ (C_6D_6 , 22 °C): δ -0.28 (s, 3H, SiMe), -0.09 (d, $^3J_{\text{P-H}} = 3.8$ Hz, 3H, SiMe), 1.32 (s, 9H, *para*-Bu), 1.64 (br s, 18H, *ortho*-Bu), 1.80 (s, 6H, C_5Me_4), 1.95 (s, 3H, C_5Me_4), 1.99 (s, 3H, C_5Me_4), 3.12 (br s, 1H, $\text{C}_5\text{Me}_4\text{H}$), 4.45 (d, $J_{\text{P-H}} = 215$ Hz, 1H, PH), 7.45 (d, $^4J_{\text{P-H}} = 2.2$ Hz, 2H, C_6H_2). $^{13}\text{C NMR}$ (C_6D_6 , 22 °C): δ -1.84 (s, 1C, SiMe₂), -1.71 (s, 1C, SiMe₂), 11.33 (s, 1C, C_5Me_4), 11.39 (s, 1C, C_5Me_4), 14.89 (s, 2C, C_5Me_4), 31.58 (s, 3C, CMe_3), 33.64 (s, 6C, CMe_3), 34.81 (s, 1C, *para*- CMe_3), 38.27 (s, 2C, *ortho*- CMe_3), 55.75 (s, 1C, *ipso*- C_5Me_4), 121.57 (d, 2C, $J_{\text{P-C}} = 3.0$ Hz, *meta*- C_6H_2), 130.21 (d, 1C, $J_{\text{P-C}} = 35.0$ Hz, *ipso*- C_6H_2), 132.97 (d, $J_{\text{P-C}} = 19.8$ Hz, *ortho*- C_6H_2), 136.61 (d, $J_{\text{P-C}} = 7.6$ Hz, *para*- C_6H_2), 147.79 (s, 2C, C_5Me_4), 154.92 (s, 2C, C_5Me_4). $^{31}\text{P NMR}$ (C_6D_6 , 22 °C): δ -131.2 (d, $J_{\text{P-H}} = 215$ Hz). Anal. Calcd for $\text{C}_{29}\text{H}_{49}\text{PSi}$: C, 76.26; H, 10.81. Found: C, 76.31; H, 11.01.

[Me₂Si(C₅Me₄)(PC₆H₂Bu₃-2,4,6)K₂(thf)_n]₂ (2**, *n* = 4; **2'**, *n* = 2).** BuLi (2.52 M, 14.8 mL, 37.30 mmol) was added to a THF solution (40 mL) of **1** (7.71 g, 16.88 mmol) at -78 °C. The resulting mixture was warmed to room temperature and stirred for 2 h. *t*BuOK (4.16 g, 37.07 mmol) was then added. After the mixture was stirred for 2 days, the solvent was removed under vacuum. The residue was washed with hexane to remove *t*BuOLi and dried under vacuum for 1 h to yield orange powder of **2'** (**2**-4THF) (10.12 g, 7.47 mmol, 88% yield). Large orange prisms of **2** could be grown from a concentrated THF solution. $^1\text{H NMR}$ ($\text{C}_5\text{D}_5\text{N}$, 22 °C) (**2'**): δ 0.56 (s, 12H, SiMe), 1.45 (s, 18H, *para*-Bu), 1.60 (q, $J = 3.23$ Hz, 16H, THF), 2.17 (s, 12H, C_5Me_4), 2.30 (s, 36H, *ortho*-Bu), 2.60 (s, 12H, C_5Me_4), 3.63 (q, $J = 3.23$ Hz, 16H, THF), 7.48 (s, 4H, C_6H_2). $^{13}\text{C NMR}$ ($\text{C}_5\text{D}_5\text{N}$, 22 °C): δ 8.29 (s, 1C, SiMe₂), 8.38 (s, 1C, SiMe₂), 11.99 (s, 2C, C_5Me_4), 15.35 (s, 1C, C_5Me_4), 15.40 (s, 1C, C_5Me_4), 25.84 (s, 2C, THF), 32.27 (s, 3C, CMe_3), 34.61 (s, 1C, *para*- CMe_3), 34.86 (s, 3C, CMe_3), 35.01 (s, 3C, CMe_3), 39.68 (s, 2C, *ortho*- CMe_3), 67.87 (s, 2C, THF), 111.21 (s, 2C, C_5Me_4), 116.48 (s, 2C, C_5Me_4), 117.81 (s, 2C, *meta*- C_6H_2), 135.91 (s, 1C, *ipso*- C_5Me_4), 141.20 (s, 1C, *para*- C_6H_2), 155.40 (d, 1C, $J_{\text{P-C}} = 73.3$ Hz, *ipso*- C_6H_2), 157.31 (s, 2C, *ortho*- C_6H_2). $^{31}\text{P NMR}$ ($\text{C}_5\text{D}_5\text{N}$, 22 °C): δ -124.4 (s). Anal. Calcd for $\text{C}_{90}\text{H}_{158}\text{K}_4\text{O}_8\text{P}_2\text{Si}_2$ (**2**): C, 65.80; H, 9.69; for $\text{C}_{74}\text{H}_{126}\text{K}_4\text{O}_4\text{P}_2\text{Si}_2$ (**2**-4THF): C, 65.63; H, 9.38; for $\text{C}_{58}\text{H}_{94}\text{K}_4\text{P}_2\text{Si}_2$ (**2**-8THF): C, 65.36; H, 8.89. Found: C, 64.24-64.83, H, 9.58-9.51. The low value of the observed carbon content was probably due to formation of incombustible carbide species.²⁶

Me₂Si(C₅Me₄)(PC₆H₂Bu₃-2,4,6)Sm(thf)_n (3**, *n* = 3; **3'**, *n* = 1).** To a dark blue THF solution (15 mL) of $\text{SmI}_2(\text{thf})_2$ (0.548 g, 1 mmol) was added **2'** (0.677 g, 0.5 mmol), which resulted in immediate formation of a cloudy dark brown solution. After the mixture was stirred for 45 min, toluene (7 mL) was added and was then stirred for 5 min to fully precipitate KI. After filtration and evaporation of the solvent, the residue was dissolved in THF. The THF solution was concentrated under reduced pressure, and hexane was layered to precipitate dark crystals of **3**, which after being dried under vacuum for 3 h yielded **3'** (**3**-2THF) as a brown powder (0.447 g, 0.660 mmol, 66% yield). $^1\text{H NMR}$ ($\text{C}_4\text{D}_8\text{O}$, 22 °C): δ -1.53 (br s, 6H, SiMe), 1.36 (br s, 6H, C_5Me_4), 1.94 (br s, 9H, *para*-Bu), 3.21 (br s, 6H, C_5Me_4), 4.55 (br s, 18H, *ortho*-Bu), 7.73 (br s, 2H, C_6H_2). $^1\text{H NMR}$ ($\text{C}_5\text{D}_5\text{N}$, 22 °C): δ -0.60 (br s, 6H, SiMe), 0.31 (br s, 6H, C_5Me_4), 1.60 (q, $J = 3.23$ Hz, 4H, THF), 2.11 (br s, 9H,

para-Bu), 2.19 (br s, 6H, C_5Me_4), 3.64 (q, $J = 3.23$ Hz, 4H, THF), 4.72 (br s, 18H, *ortho*-Bu), 8.36 (br s, 2H, C_6H_2). Anal. Calcd for $\text{C}_{41}\text{H}_{71}\text{O}_3\text{PSiSm}$ (**3**): C, 59.95; H, 8.71; for $\text{C}_{33}\text{H}_{55}\text{OPSiSm}$ (**3**-2THF): C, 58.53; H, 8.19; for $\text{C}_{29}\text{H}_{47}\text{PSiSm}$ (**3**-3THF): C, 57.56; H, 7.83. Found: C, 52.84-53.31, H, 7.55-7.59. The low value of the observed carbon content was probably due to formation of incombustible carbide species.²⁶

Me₂Si(C₅Me₄)(PC₆H₂Bu₃-2,4,6)Yb(thf)₃ (4**, *n* = 3; **4'**, *n* = 0).** Addition of **2'** (0.772 g, 0.57 mmol) to a THF solution (20 mL) of $\text{YbI}_2(\text{thf})_2$ (0.651 g, 1.14 mmol) gave immediately a cloudy orange solution. The solution was stirred for 45 min and the solvent was removed under vacuum. Addition of toluene to the orange residue resulted in formation of a bright green solution with precipitation of KI. After filtration and evaporation of the solvent under vacuum, a green oily residue was obtained, which after being washed with hexane and dried under vacuum yielded **4'** (**4**-3THF) as a green powder (0.579 g, 0.92 mmol, 81% yield). Orange needlelike crystals of **4** could be obtained from a saturated THF solution. Leaving **4** under vacuum for 2 h regenerated **4'**. $^1\text{H NMR}$ ($\text{C}_5\text{D}_5\text{N}$, 22 °C): δ 0.64 (s, 6H, SiMe), 1.42 (s, 9H, *para*-Bu), 2.08 (s, 6H, C_5Me_4), 2.13 (br s, 24H, *ortho*-Bu, C_5Me_4), 7.50 (s, 2H, C_6H_2). $^1\text{H NMR}$ ($\text{C}_4\text{D}_8\text{O}$, 22 °C): δ 0.05 (s, 6H, SiMe), 1.26 (s, 9H, *para*-Bu), 1.73 (s, 18H, *ortho*-Bu), 1.95 (s, 6H, C_5Me_4), 2.15 (s, 6H, C_5Me_4), 7.03 (s, 2H, C_6H_2). $^{31}\text{P NMR}$ ($\text{C}_5\text{D}_5\text{N}$, 22 °C): δ -113.5 (s with ^{171}Yb satellites, $J_{\text{P-Yb}} = 992$ Hz). Anal. Calcd for $\text{C}_{41}\text{H}_{71}\text{O}_3\text{PSiYb}$ (**4**): C, 58.34; H, 8.48; for $\text{C}_{29}\text{H}_{47}\text{PSiYb}$ (**4**-3THF): C, 55.48; H, 7.55. Found: C, 48.01-49.84; H, 7.31-7.41. The low value of the observed carbon content was probably due to formation of incombustible carbide species.²⁶

Me₂Si(C₅Me₄)(PC₆H₂Bu₃-2,4,6)Sm(hmpa)₂ (5**).** Addition of HMPA (52 μL , 0.296 mmol) to **3'** (0.100 g, 0.148 mmol) in toluene (5 mL) gave a dark green solution. After evaporation of the solvent under vacuum, the residue was washed with hexane and dried to yield **5** as pale green powder (0.134 g, 0.139 mmol, 94%). Cubic dark green crystals of **5** were grown in a saturated toluene solution in a few days. $^1\text{H NMR}$ ($\text{C}_5\text{D}_5\text{N}$, 22 °C): δ -1.04 (br s, 6H, SiMe), 0.77 (br s, 6H, C_5Me_4), 2.06 (br s, 9H, *para*-Bu), 2.21 (br d, $J_{\text{P-H}} = 8.70$ Hz, 36H, NMe), 2.79 (br s, 6H, C_5Me_4), 4.76 (br s, 18H, *ortho*-Bu), 8.27 (br s, 2H, C_6H_2). $^1\text{H NMR}$ (C_6D_6 , 22 °C): δ -4.53 (br s, 6H, SiMe), 0.06 (br s, 36H, NMe); 2.67 (br s, 9H, *para*-Bu), 6.86 (br s, 6H, C_5Me_4), 8.36 (br s, 18H, *ortho*-Bu), 9.55 (br s, 2H, C_6H_2), 14.73 (br s, 6H, C_5Me_4). Anal. Calcd for $\text{C}_{41}\text{H}_{83}\text{N}_6\text{O}_2\text{P}_3\text{SiSm}$ (**5**): C, 51.11; H, 8.68. Found: C, 48.08-50.17; H, 8.47-8.65. The low value of the observed carbon content was probably due to formation of incombustible carbide species.²⁶

Me₂Si(C₅Me₄)(PC₆H₂Bu₃-2,4,6)Sm(dme)₂ (6**).** Dissolving of **3'** (0.100 mg, 0.148 mmol) in dimethoxyethane (DME) gave a dark brown solution. After removal of the solvent under vacuum, the residue was washed with hexane and dried to yield **6** as a dark brown powder (0.096 g, 0.122 mmol, 83% yield). Black cubic crystals of **6** were obtained by layering of hexane to a concentrated DME solution. $^1\text{H NMR}$ ($\text{C}_5\text{D}_5\text{N}$, 22 °C): δ -0.74 (br s, 6H, SiMe), 0.13 (br s, 6H, C_5Me_4), 2.08 (br s, 9H, *para*-Bu), 2.25 (br s, 6H, C_5Me_4), 3.28 (s, 12H, OMe), 3.47 (s, 8H, OCH_2), 4.65 (s, 18H, *ortho*-Bu), 8.27 (s, 2H, C_6H_2). $^1\text{H NMR}$ ($\text{C}_4\text{D}_8\text{O}$, 22 °C): δ -1.65 (br s, 6H, SiMe), 1.15 (br s, 6H, C_5Me_4), 1.98 (br s, 9H, *para*-Bu), 2.70 (br s, 6H, C_5Me_4), 2.83 (s, 8H, OCH_2), 4.31 (s, 12H, OMe), 4.73 (br s, 18H, *ortho*-Bu), 7.80 (br s, 2H, C_6H_2). Anal. Calcd for $\text{C}_{37}\text{H}_{67}\text{O}_4\text{PSiSm}$ (**6**): C, 56.59; H, 8.60. Found: C, 53.34-53.54; H, 8.27-8.42. The low value of the observed carbon content was probably due to formation of incombustible carbide species.²⁶

[Me₂Si(C₅Me₄)(PC₆H₂Bu₃-2,4,6)Sm(thf)₂(μ - η^2 -OCPh₂)₂·THF (7**·THF).** To **3'** (0.272 g, 0.402 mmol) was added benzophenone (0.037 g, 0.201 mmol) in THF (10 mL). The resulting green solution was stirred at room temperature for 1 h. After reduction of the solution volume under reduced pressure, hexane was layered to give **7**·THF as dark green crystals, which after being dried, yielded **7** (0.200 g, 0.129

(26) Failure in obtaining satisfactory microanalytical data for some lanthanide complexes bearing P atom-containing ligands was also mentioned previously by other groups. For examples, see: (a) Nief, F.; Ricard, L. *J. Organomet. Chem.* **1994**, *464*, 149; **1997**, *529*, 357. (b) Rabe, G. W.; Ziller, J. W. *Inorg. Chem.* **1995**, *34*, 5378. (c) Gröb, T.; Seybert, G.; Massa, W.; Weller, F.; Palaniswami, R.; Greiner, A.; Dhnicke, K. *Angew. Chem., Int. Ed.* **2000**, *39*, 4373. See also refs 4, 11d.

mmol, 64% yield). ^1H NMR ($\text{C}_5\text{D}_5\text{N}$, 22 °C): δ -1.06 (s, 3H, SiMe), -0.50 (s, 3H, SiMe), 1.39 (s, 9H, tBu), 1.47 (s, 9H, tBu), 1.50 (s, 9H, tBu), 1.52 (s, 3H, C_5Me_4), 1.61 (q, $J = 3.08$ Hz, 4H, THF), 1.83 (s, 3H, C_5Me_4), 1.98 (s, 3H, C_5Me_4), 2.24 (s, 3H, C_5Me_4), 3.64 (q, $J = 3.08$ Hz, 4H, THF), 7.38 (s, 1H, C_6H_2), 7.53 (s, 1H, C_6H_2), 7.63 (t, $J = 7.5$ Hz, 1H, Ph), 7.75 (t, $J = 7.5$ Hz, 2H, Ph), 9.48 (d, $J = 7.5$ Hz, 2H, Ph). Anal. Calcd for $\text{C}_{79}\text{H}_{120}\text{O}_3\text{P}_2\text{Si}_2\text{Sm}_2$ (**7**): C, 61.75; H, 7.87. Found: C, 57.42–59.30; H, 7.77–7.88. The low value of the observed carbon content was probably due to formation of incombustible carbide species.²⁶

[Me₂Si(C₅Me₄)(PC₆H₂¹Bu₃-2,4,6)Sm(μ -I)(thf)]₂ (8**).** A toluene solution (30 mL) of $\text{ICH}_2\text{CH}_2\text{I}$ (0.200 g, 0.709 mmol) was slowly added to **3'** (0.904 g, 1.335 mmol). The resulting dark orange solution was stirred at room temperature for 4 h. Removal of the solvent under vacuum afforded a pale orange residue, which was washed with hexane and dried under vacuum to give **8** as an orange powder (0.840, 0.522 mmol, 78% yield). Orange crystals of **8** were obtained from benzene/hexane. ^1H NMR ($\text{C}_5\text{D}_5\text{N}$, 22 °C): δ 0.42 (s, 6H, SiMe), 1.27 (s, 9H, *para*-Bu), 1.36 (s, 18H, *ortho*-Bu), 1.60 (m, 4H, THF), 1.64 (s, 6H, C_5Me_4), 1.77 (s, 6H, C_5Me_4), 3.64 (m, 4H, THF), 7.08 (s, 2H, C_6H_2). ^1H NMR (C_6D_6 , 22 °C): δ -1.60 (br s, 6H, SiMe), -0.39 (br s, 18H, *ortho*-Bu), 0.33 (br s, 6H, C_5Me_4), 1.23 (m, 4H, THF), 1.38 (s, 9H, *para*-Bu), 1.61 (s, 6H, C_5Me_4), 2.00 (m, 4H, THF), 7.27 (s, 2H, C_6H_2). Anal. Calcd for $\text{C}_{66}\text{H}_{110}\text{O}_2\text{P}_2\text{Si}_2\text{Sm}_2$: C, 49.29; H, 6.89. Found: C, 48.66–48.75; H, 6.85–6.89. The low value of the observed carbon content was probably due to formation of incombustible carbide species.²⁶

X-ray Crystallographic Studies. Crystals for X-ray analyses were obtained as described in the preparations. The crystals were manipulated in the glovebox under a microscope mounted on the glovebox window and were sealed in thin-walled glass capillaries. Data collections for **1**, **2**, **5**, and **6** were performed at 20 °C on a Rigaku RAXIS CS imaging plate diffractometer with graphite-monochromated Mo K α radiation ($\lambda = 0.71070$ Å). The structures of **1**, **2**, **5**, and **6** were solved by using the teXsan software package. Data collections for **4**, **7**, and **8** were performed at 20 °C on a Bruker SMART APEX diffractometer with a CCD area detector, using graphite-monochromated Mo K α radiation ($\lambda = 0.71069$ Å). The determination of crystal class and unit cell parameters was carried out by the SMART program package. The raw frame data were processed using SAINT and SADABS to yield the reflection data file. The structures of **4**, **7**, and **8** were solved by using the SHELXTL program. Refinements were performed on F for **1**, **2**, **5**, and **6** and on F^2 for **4**, **7**, and **8** anisotropically for all non-hydrogen atoms by the full-matrix least-squares method. The hydrogen atom on the P atom in **1** was located from the difference Fourier map and was refined isotropically. Other hydrogen atoms were placed at the calculated positions and were included in the structure calculation without further refinement of the parameters. The residual electron densities were of no chemical significance. Crystal data and processing parameters are summarized in Table 2.

Polymerization of Ethylene. In the glovebox, **3'** (34 mg, 0.05 mmol), a magnetic stir bar, and toluene (15 mL) were placed in a 100 mL three-neck flask. The flask was taken outside, set in a water bath (25 °C), and then connected to a Schlenk line, a well-purged ethylene line, and a mercury-sealed stopper. Introduction of ethylene resulted in immediate formation (precipitation) of polyethylene. The mixture was stirred for 15 min, during which a slightly positive ethylene pressure was maintained by the stopper. MeOH (20 mL) was added. The resultant mixture was poured into 300 mL of MeOH in a 1 L beaker and then stirred to further precipitate the polymer product. After filtration, the polymer product was dried under vacuum in an oven (80 °C) overnight, yielding 170 mg of polyethylene. Characterization of this polymer was

Table 2. Summary of Crystallographic Data

	1	2	4	5	6	7-2THF	8
formula	$\text{C}_{29}\text{H}_{49}\text{P}\text{Si}$	$\text{C}_{90}\text{H}_{158}\text{O}_8\text{K}_4\text{Si}_2\text{P}_2$	$\text{C}_{41}\text{H}_{71}\text{O}_3\text{P}_3\text{SiYb}$	$\text{C}_{41}\text{H}_{83}\text{N}_6\text{O}_2\text{P}_3\text{SiSm}$	$\text{C}_{71}\text{H}_{134}\text{O}_8\text{P}_2\text{Si}_2\text{Sm}_2$	$\text{C}_{87}\text{H}_{136}\text{O}_3\text{P}_2\text{Si}_2\text{Sm}_2$	$\text{C}_{66}\text{H}_{110}\text{O}_2\text{P}_2\text{Si}_2\text{Sm}_2$
fw	456.77	1642.75	844.08	963.55	1570.78	1680.78	1608.16
cryst syst	monoclinic	triclinic	monoclinic	monoclinic	monoclinic	monoclinic	monoclinic
space group	$\text{P}2_1/\text{n}$ (No. 14)	$\text{P}\bar{1}$ (No. 2)	$\text{P}2_1/\text{c}$ (No. 14)	$\text{P}2_1/\text{n}$ (No. 14)	$\text{P}2_1/\text{a}$ (No. 14)	$\text{C}2/\text{c}$ (No. 15)	$\text{C}2/\text{c}$ (No. 15)
a (Å)	13.903(7)	14.346(8)	22.719(4)	12.008(1)	17.618(3)	37.532(3)	24.266(3)
b (Å)	15.215(2)	15.104(7)	12.874(2)	32.733(8)	18.825(7)	10.0717(8)	14.783(2)
c (Å)	14.383(2)	13.638(2)	17.296(3)	13.679(5)	27.104(4)	27.996(2)	21.254(2)
α (deg)	101.151(3)	99.56(3)	106.249(3)	98.198(9)	101.74(1)	124.488(1)	101.568(2)
β (deg)	2985(1)	98.38(3)	4857(2)	5321(2)	8801(3)	8723(1)	7469(1)
γ (deg)	4	114.34(5)	4	4	4	4	4
V (Å ³)	1.016	2578(2)	1.154	1.203	1.185	1.280	1.430
Z	1.45	1	20.12	12.54	14.32	14.44	24.95
D_c (g/cm ³)	5754	6942	24755	10142	20489	33311	27928
μ (cm ⁻¹)	3703 (x = 3)	3652 (x = 3)	12526 (x = 2)	7774 (x = 3)	14352 (x = 3)	12163 (x = 2)	10452 (x = 2)
no. of reflns colld	284	479	439	488	795	458	358
with $I_o > x\sigma(I_o)$	2.475 (F)	2.74 (F)	0.829 (F ²)	1.97 (F)	1.59 (F)	0.743 (F ²)	0.876 (F ²)
GOF	0.075	0.094	0.0748	0.063	0.053	0.0346	0.0590
R	0.099	0.110	0.1943	0.093	0.075	0.0644	0.0995
R _w							

difficult because of its low solubility (insoluble in *ortho*-dichlorobenzene even at 135 °C).

Polymerization of ϵ -Caprolactone (CL). In the glovebox, **3'** (14 mg, 0.02 mmol) was dissolved in 20 mL of toluene in a two-neck flask which was equipped with a magnetic stir bar and a dropping funnel containing 2.28 g of CL (20 mmol). The flask was taken outside and connected to a Schlenk line. CL was added through the funnel with vigorous stirring. The color of the mixture changed immediately from brown to pale yellow, and the resulting pale yellow solution quickly became viscous. The magnetic stirring was ceased within a minute owing to the viscosity. After 10 min, methanol was added to precipitate poly(CL), which after filtration was dried at 60 °C overnight and weighted (2.28 g, 100% yield). The molecular weight and molecular weight distribution of the polymer were determined at 40 °C against polystyrene standard by gel permeation chromatography (GPC) on a Shodex GPC System-11 apparatus with two KF 805L columns. THF was used as an eluent.

Polymerization of 1,3-Butadiene. In the glovebox, **3'** (7 mg, 0.01 mmol) and toluene (6.7 mL) were placed in a glass pressure-reactor. The reactor was taken out from the glovebox, and MMAO (2.09 mmol, 1.1 mL \times 1.9 M in toluene obtained from Tosoh Finechem Co.) was added. The mixture was stirred for 5 min at room temperature to give a wine-red solution.

The reactor was cooled to -78 °C, and butadiene (2.2 mL, 1.35 g, 25 mmol) was then introduced. The resulting pale yellow solution was warmed to 50 °C and stirred vigorously for 80 min. The polymerization was terminated by pouring the mixture into a large quantity of methanol containing a small amount of hydrochloric acid (ca. 0.5 M) and butylhydroxytoluene (BHT) as a stabilizer agent. The polymer was isolated by decantation and dried under reduced pressure at 60 °C overnight (0.877 g, 65% yield). The microstructure of the polymer was measured by ^1H NMR and ^{13}C NMR spectroscopy in CDCl_3 . The molecular weight and molecular weight distribution were determined at 40 °C against a polystyrene standard by GPC on a Shodex GPC System-11 apparatus.

Acknowledgment. This work was partly supported by a grant-in-aid from the Ministry of Education, Culture, Sports, Science and Technology, Japan.

Supporting Information Available: Tables of atomic coordinates, thermal parameters, and bond distances and angles for **1**, **2**, and **4–8**. This material is available free of charge via the Internet at <http://pubs.acs.org>.

OM010469I